AIRBORNE LIDAR FEATURE SELECTION FOR URBAN CLASSIFICATION USING RANDOM FORESTS

Nesrine Chehata[1,2], Li Guo[1], Clément Mallet[2]

[1] Institut EGID, University of Bordeaux, GHYMAC Lab:
1 allée F.Daguin, 33607 Pessac, France.
[1] Institut Géographique National, MATIS Lab:
2-4 avenue pasteur, 94165 St Mandé, France.

Commission III - WG III/2

KEY WORDS: Lidar, Full-waveform, Classification, Feature selection, Random Forests, Urban scenes

ABSTRACT:

Various multi-echo and Full-waveform (FW) lidar features can be processed. In this paper, multiple classifers are applied to lidar feature selection for urban scene classification. Random forests are used since they provide an accurate classification and run efficiently on large datasets. Moreover, they return measures of variable importance for each class. The feature selection is obtained by backward elimination of features depending on their importance. This is crucial to analyze the relevance of each lidar feature for the classification of urban scenes. The Random Forests classification using selected variables provide an overall accuracy of 94.35%.

1 INTRODUCTION

Airborne lidar systems have become an alternative source for the acquisition of altimeter data providing unstructured 3D point clouds that describe the Earth's topography. The altimeter accuracy of a topographic lidar measurement is high (<0.1 m). Depending on the geometry of illuminated surfaces, several backscattered echoes can be recorded for a single pulse emission. Many authors have shown the potential of multi-echo lidar data for urban area analysis and building extraction (Sithole and Vosselman, 2004). 3D point cloud classification can be based on geometric and textural attributes (Matikainen et al., 2007). Other works include the lidar intensity (Charaniya et al., 2004) or combine lidar and multispectral data (Secord and Zakhor, 2007, Rottensteiner et al., 2005). Since 2004, full-waveform (FW) lidar systems have emerged with the ability to record the complete waveform of the backscattered 1D-signal laser pulse. In (Gross et al., 2007, Wagner et al., 2008), FW lidar features were used to detect vegetated areas. In urban scenes, the potential of such data has been barely investigated. For the analysis of laser scanner data, various classification techniques have been applied such as unsupervised classification by ISODATA (Haala and Brenner, 1999) and supervised classification as Bayesian networks (Stassopoulou et al., 2000), Dempster shafer fusion theory (Rottensteiner et al., 2005), Support Vector Machines (Secord and Zakhor, 2007, Charaniya et al., 2004, Mallet et al., 2008) or classification trees (Ducic et al., 2006, Matikainen et al., 2007).

In this work, we study different lidar features, multiecho and full-waveform to classify urban scenes into four classes: Buildings, vegetation, natural ground and artificial ground. Artificial ground gathers all kinds of streets and street items such as cars, traffic lights whereas the natural ground includes grass, sand, and bare-earth regions. No filtering is applied before the classification. The objective is to select the most relevant features for classifying urban scenes and to provide an accurate classification with a small number of features. We propose to achieve both objectives using Random Forests. It is an ensemble classifier based on decision trees. It returns good classfication results and provides also feature selection.
The paper is organized as follows. The lidar features will be detailed in Section 2. In Section 3, multiple classifiers are presented and especially Random Forests. The feature selection process is detailed in Section 3.3. Experimental results are then discussed in Section 4 and finally, conclusions are drawn in Section 5.

2 AIRBORNE LIDAR FEATURES

Multi-echo and full-waveform lidar data are available. The feature vector is composed of 21 components: 17 multi-echo and 4 full-waveform lidar features. The multi-echo lidar features are separated into height-based, echo-based, eigenvalue-based and local 3D-plane based features. The resulting feature vector fv for each site is given by:

$$fv = [\Delta z\ \Delta z_{fl}\ \sigma_z^2\ \mathcal{C};\ N\ N_e\ ;\ \lambda_1\ \lambda_2\ \lambda_3\ A_\lambda\ P_\lambda\ S_\lambda\ L_\lambda;\ N_z\ \sigma_{N_z}^2\ \mathcal{R}_z\ D_\Pi;\ A\ w\ \sigma\ \alpha]^T$$

All these features are computed using a volumetric approach within a local neighborhood $\mathcal{V}_P$ at each lidar point P. The local neighborhood includes all the lidar points within a cylinder, with a fixed radius, centered at the point. Lidar points are then projected into a 2D image geometry (0.5 m resolution). Feature images are obtained by computing, for each pixel, the mean corresponding value of the lidar points included in a 3×3 raster kernel (*cf.* Figure. 1). Table 1 summarizes input lidar features which are separated into five groups. Lidar features are detailed hereby.

2.1 Height-based lidar features

The first group is based on 3D point heights:

- Δz: Height difference between the lidar point and the lowest point found in a large cylindrical volume whose radius has been experimentally set to 15 m. This feature will help discriminating ground and off-ground objects (*cf.* Figure. 1(b)).
- Δz_{fl}: Height difference between First and Last pulses of the waveform of the current lidar point. It helps discriminating building roofs and ground.
- σ_z^2: The height variance. This feature has high values for vegetation (*cf.* Figure. 1(c)).

- $\mathcal{C}$: The local curvature is a discrete version of the Laplace operator. It is the maximum value of the gradient differences on heights, which are computed in four main directions based on a raster grid (Steinle and Vögtle, 2001). A 3×3 raster kernel has been chosen.

2.2 Echo-based features

- N: Total number of echoes within the waveform of the current lidar point. This feature is high for vegetation and building facades.
- N_e: Normalized number of echoes obtained by dividing the echo number by the total number of echoes within the waveform of the current lidar point. This feature highlights the vegetation since multiple reflections can occur on it (*cf.* Figure. 1(d)).

2.3 Eigenvalue-based lidar features

The variance-covariance matrix is computed within the local neighborhood $(V)_P$. The Eigenvalues $\lambda_1 > \lambda_2 > \lambda_3$ are used as features. Besides, they provide additional features and help discriminating planes, edges, corners, lines, and volumes (Gross and Thoennessen, 2006). These features describe the spatial local distribution of the 3D points.

$$\text{Anisotropy} = A_\lambda = \frac{\lambda_1 - \lambda_3}{\lambda_1} \quad (1)$$

$$\text{Planarity} = P_\lambda = \frac{\lambda_2 - \lambda_3}{\lambda_1} \quad (2)$$

$$\text{Sphericity} = S_\lambda = \frac{\lambda_3}{\lambda_1} \quad (3)$$

$$\text{Linearity} = L_\lambda = \frac{\lambda_1 - \lambda_2}{\lambda_1} \quad (4)$$

λ_3 has low values for planar objects and higher values for non-planar objects (*cf.* Figure. 1(e)). The planarity feature shows high values especially for planar objects. Conversely, the sphericity feature gives high values for isotropic distributed 3D neighborhood.

2.4 Local plane-based lidar features

The planarity of the local neighboorhood will help discriminating buildings from vegetation. The local plane Π_P within $\mathcal{V}_P$ is estimated using a robust M-estimator with norm $L_{1.2}$ (Xu and Zhang, 1996).

- N_z: Deviation angle of Π_P normal vector from the vertical direction. This feature highlights the ground (*cf.* Figure.1(f)).
- σ_z^2: Variance of deviation angles within $\mathcal{V}_P$. It discriminates planar surfaces such as roads and building roofs from vegetation.
- $\mathcal{R}_\pi$: Residuals of the local plane estimated in a small vertical cylinder (0.5 m radius). Residuals $\mathcal{R}_\pi$ are calculated w.r.t the estimated plane as follows:

$$\mathcal{R}_\pi = \sum_{i \in \nu_P} \frac{(d_i)^l}{l} \quad (5)$$

where d_i is the distance between the lidar point $i \in \nu_P$ and the plane. Here l=1.2. Residuals should be high for vegetation.

- D_π: Distance from the current point P to the local estimated plane Π_P.

2.5 Full-waveform lidar features

The remaining features are more specific to FW lidar data and are obtained by modelling the lidar waveforms. The amplitude and echo width are described in (Wagner et al., 2006).

- A: echo amplitude. High amplitude values can be found on building roofs, on gravel, and on cars. Asphalt and tar streets have low values. The lowest values correspond to vegetation due to a higher target heterogeneity and attenuation (*cf.* Figure. 1(g)).
- w: echo width. Higher values correspond to vegetation since it spreads the lidar pulse. A low width is likely to correspond to ground and buildings. However, it may increase with roof slope (*cf.* Figure. 1(h)).
- α: echo shape describing how locally spread the peak is. It is obtained from a waveform decomposition based on a generalized Gaussian modeling function (Chauve et al., 2007). The authors also show that very low and high shape values correspond mainly to building roofs and vegetation.
- σ: echo cross-section corresponds more or less to the peak energy. $\sigma = A \times w$. It is the basic quantity to describe the scattering of a wave by an object. The cross-section values are high for buildings, medium for vegetation and low for artificial ground.

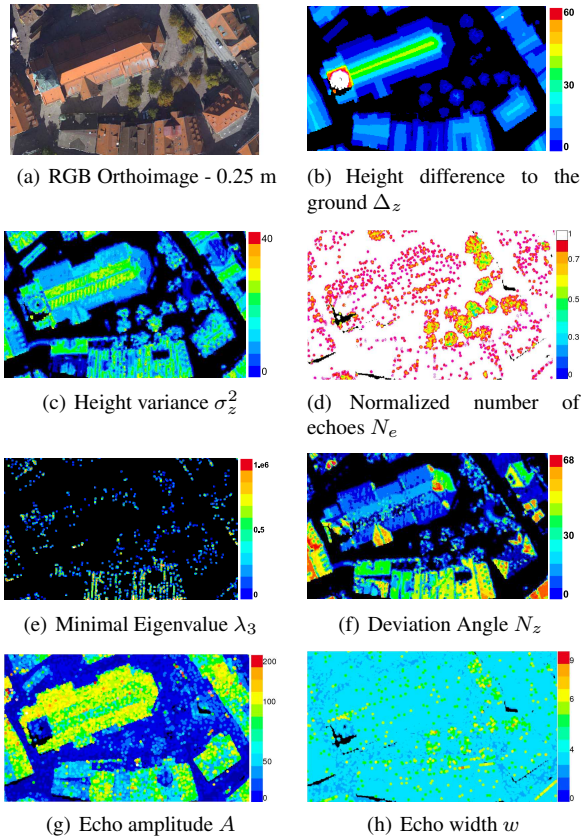

(a) RGB Orthoimage - 0.25 m (b) Height difference to the ground Δ_z

(c) Height variance σ_z^2 (d) Normalized number of echoes N_e

(e) Minimal Eigenvalue λ_3 (f) Deviation Angle N_z

(g) Echo amplitude A (h) Echo width w

Figure 1: Orthoimage and some representative Lidar features.

3 MULTIPLE CLASSIFIERS

Over the last two decades, many multiple classifiers have been proposed. Several classifiers are trained and their results combined through a voting process. In this paper, we focus on multiple classifiers that are built at data level. The modified data sets are applied to train each classifier in the ensemble, the base classifier should be unstable, that is, small changes in the training set will lead to large changes in the classifier output. Neural

Type	Symbol	Feature
Height features	Δz	Height diff. to the ground
	Δz_{fl}	Height diff. first-last echoes
	σ_z^2	Height variance
	$\mathcal{C}$	Local curvature
Echo features	N	Number of echoes
	N_e	Normalized number of echoes
Eigenvalue features	λ_1	Highest eigenvalue
	λ_2	Medium eigenvalue
	λ_3	Lowest eigenvalue
	A_λ	Anisotropy
	P_λ	Planarity
	S_λ	Sphericity
	L_λ	Linearity
Local plane features	N_z	Deviation angle
	$\sigma_{n_z}^2$	Variance of deviation angles
	$\mathcal{R}_z$	Residuals to the local plane
	D_Π	Distance to the local plane
FW Lidar features	A	Echo amplitude
	w	Echo width
	σ	Cross-section
	α	Echo shape

Table 1: Synthesis of Lidar features for classification

Networks and Decision Trees are two examples of unstable classifiers. The most widely used methods are bagging and boosting. Boosting iteratively reproduces the training set for each classifier by increasing the weight to the incorrectly classified samples in previous classifier. Bagging is the acronym of "bootstrap aggregating". It is made of the ensemble of bootstrap-inspired classifiers produced by sampling with replacement from training instances and uses these classifiers to get an aggregated classifier. It aims at reducing the variance of a classifier (Briem et al., 2002).

3.1 Random Forests

Random Forests are a variant of bagging proposed by (Breiman, 2001). It is a decision tree based ensemble classifier that has excellent performance in classification tasks comparable to boosting (Breiman, 2001), even Support Vector Machines (SVMs) (Pal, 2005). It can be used with multi-class problems. It is non-parametric and does not require assuptions on the distribution of the data. This is an interesting property when different types or scales of input attributes are used. Moreover, Random Forests run efficiently on large data sets and can handle thousands of input variables without variable deletion. They do not overfit. They have a good predictive performance even when most predictive variables are noisy. Therefore, there is no need for variable preselection (Strobl et al., 2007). In addition, Random Forests is a classification algorithm that directly provide measures of variable importance (related to the relevance of each variable in the classfication process). These outstanding features make it suitable for the classification of remote sensing data such as multispectral data (Pal, 2005) or multisource data (Gislason et al., 2006).

Random Forests are a combination of tree predictors such that each tree depends on the values of a random vector sampled independently and with the same distribution for all trees in the forest (Breiman, 2001). As in Breiman's method, in training, the algorithm creates multiple bootstrapped samples of the original training data, then builds a number of no pruning Classification and Regression Trees (CART) from each bootstrapped samples set and only a randomly selected subset of the input variables is used to split each node of CART. For classification, each tree in the Random Forests gives a unit vote for the most popular class at each input instance. The label of input instance is determined by a majority vote of the trees. The number of variables M, randomly chosen at each split, is considered as the single user-defined adjustable parameter. This parameter is not critical and is often set to the square root of the number of inputs (Gislason et al., 2006).

In this work, Random Forests are applied to classify airborne lidar data on urban scenes and to select the most important features for this task. This avoids the user to manually select relevant attributes. Random Forests have not yet been used with airborne lidar data.

3.2 Variable importance

Aside from classification, Random Forests provide measures of variable importance based on the permutation importance measure which was shown to be a reliable indicator (Strobl et al., 2007).When the training set for a particular tree is drawn by sampling with replacement, about one-third of the cases are left out of the sample set. These out-of-bag (OOB) data can be used to estimate the test accuracy and the permutation importance measure. The importance of variable m can be estimated by randomly permuting all the values of the m^{th} variable in the OOB samples for each tree. A measure for variable importance (Breiman, 2001) can be the difference in prediction accuracy (i.e. the number of observations classified correctly) before and after permuting variable m, averaged over all trees. A high decrease of prediction accuracy indicates the importance of that variable.

3.3 Feature selection

The objective of feature selection is to identify small sets of lidar features that can still achieve a good predictive performance and so that correlated features should not be selected. In this paper, we use a backward elimination of features using OOB errors. This feature selection process was proposed in (Díaz-Uriarte and de Andrés, 2006), for biological application, to select genes of microarray data. Using data simulations, the authors showed its robustness to noise or redundant features.

To select the most relevant features, we iteratively fit Random Forests. At each iteration, a fraction of the features (the least important ones) is eliminated and a new forest is built. By default, the fraction is fixed to 0.2. It allows a relatively fast operation, and increases the resolution as the number of considered features becomes smaller. After fitting all forests, the selected set of features is the one whose OOB error rate is within u = 1 standard error of the minimum error rate of all forests. This is similar to the "s.e. rule" commonly used in classification trees literature (Breiman et al., 1984). This strategy can lead to solutions with fewer features while achieving an error rate that is not different, within sampling error, from the best solution.

4 EXPERIMENTAL RESULTS

4.1 Data set

The data acquisition was carried out with the RIEGL LMS-Q560 system over the city of Biberach (Germany). The main technical characteristics of this sensor are presented in (Wagner et al., 2006) and summarized in Table 2.

The city of Biberach includes artificial grounds, natural grounds, vegetation and buildings. This lidar data set has been used for classifying urban scenes using Support Vector Machines (Mallet

Flight height	Footprint size	PRF	Pulse density
500 m	0.25 m	100 KHz	2.5 (pt/m^2)

Table 2: Specifications of Biberach data set.

et al., 2008) with fewer features. The number of available reference samples is 797364 and they are split almost evenly between training and test samples.

Class	Training samples	Test samples
Buildings	187673	188015
Vegetation	15982	15723
Nat. Ground	2174	2149
Art. Ground	192704	192944
Total samples	398533	398831

Table 3: Data Set.

4.2 Variable importance results

The variable importance estimate for the training data is depicted on Figure 2 for each group feature. Considering all classes, it is obtained by the mean decrease permutation accuracy. The

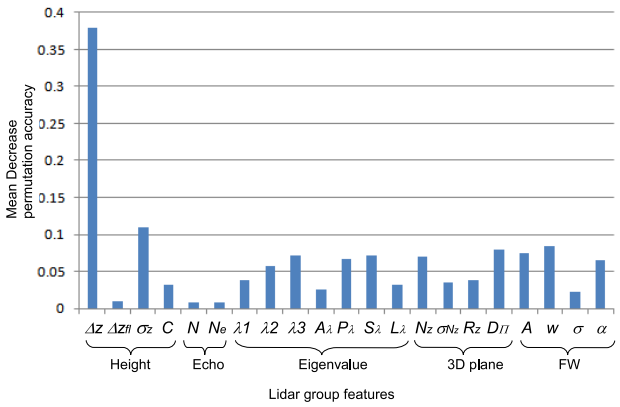

Figure 2: Variable importance of Lidar data by mean decrease permutation accuracy.

most important features are height-based: the height difference and the height variance. Echo-based features are not important for urban scene classification when using other attributes that describe more accurately the local distribution of 3D points such as eigenvalue-based or 3D plane-based features. Moreover, the First-Last height difference is not important to classify urban objects since it is used with the height variance σ_z^2. In fact, both variables can be correlated and the latter has more values which allows to distinguish rooftops building and ground for instance.

As for the eigenvalue-based features, λ_3 is the most important eigenvalue, as expected. In fact, it returns the lowest values for planar objects. The sphericity S_λ shows a high importance whereas the correlated anisotropy feature A_λ shows a lower one. This illustrates the advantage of permutation accuracy measure since redundant features should be less important. Among 3D-plane based features, the distance to plane D_Π seems to be the most important one. Finally, for full-waveform features, echo amplitude, and width are the most important for all classes. The FW cross-section σ is less important as it is correlated to the former features.

4.3 Feature selection results

To fix the Random Forests parameters, (Díaz-Uriarte and de Andrés, 2006) showed that the relation of OOB rate with the number of split variables M is largely independent of the number of trees T (for T between 1000-40000). In addition, the default setting of M is a good choice of OOB rate. Therefore, the feature selection was run with $M = 4$ and $T = 1000$ trees. Figure 3 is obtained by the backward iterative elimination of features using OOB errors. The graph is shown in a forward way to illustrate the more relevant features. On the x-axis, eigenvalue and FW Lidar features appear respectively in blue and red colors. The selection

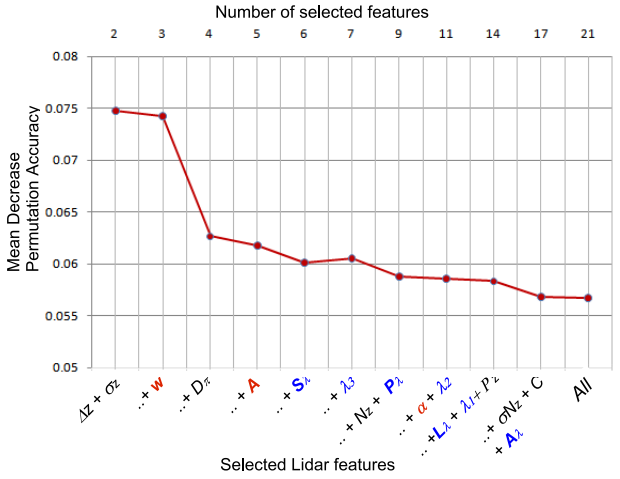

Figure 3: Iterative elimination Lidar feature selection.

process returns a feature vector of 17 attributes, where $\Delta_{z_{fl}}$, N, N_e and σ are eliminated. Another strategy may consist in keeping the set which first makes the variable importance decrease. In our case the final set may corresponds [Δ_z,σ_z,w,D_Π,A,S_λ]. The corresponding total error is 6%. One can observe that four feature groups are represented: the height based group is the most important one, then two FW features are selected which confirms the contribution of full-waveform lidar data for urban scene classification.

4.4 Classification results

Based on the 17 selected features, the Random Forests classification was run and variable importance computed for each class. Underlying parameters have been fixed to $M = 4$ which means that four variables are considered at each split and the number of trees was set experimentally to 60. The study area is visible on figure 4. We observe that errors occur mainly on building edges. The corresponding lidar points might be ambiguous since they correspond to transition points between building and artificial ground classes. Besides, these confusion errors are amplified due to the interpolation process of lidar points in 2D geometry.

The confusion matrix for test data is given in Table 4. The raster neighborhood size is 3×3. Artificial ground and buildings are well classified with lower error rate. However, the algorithm has more difficulties in classifying natural ground and vegetation. The former class suffers from smaller training set than the other classes. As for vegetation, confusions essentially occur with artificial ground due to the lidar data interpolation. In fact, in non-dense vegetated areas, the lidar beam is likely to reach the ground underneath and the resulting waveform has mixed properties. Therefore, some lidar feature pixels may be a combination of both classes.

4.4.1 2D Geometry impact Since lidar features are processed in a 2D geometry, we studied the effect of the neighborhood size on classification and variable importance results. A neighborhood size of 5×5 was tested. The corresponding confusion matrix is illustrated in Table 5.

Class	Art.Grnd	Build.	Nat.Grnd	Veget.	Error %
Art.Grnd	188562	3325	5	1052	2.3
Build.	13946	173545	5	519	7.7
Nat.Grnd	500	20	1622	7	24.5
Veget.	2604	566	0	12553	20.2

Table 4: Confusion matrix for test data using 60 trees and 4 split variables. Total error rate=5.65%, 3×3 window size

Class	Art.Grnd	Build.	Nat.Grnd	Veget.	Error %
Art.Grnd	186047	5483	33	1381	3.6
Build.	7364	180154	2	495	4.2
Nat.Grnd	1403	33	703	10	67.3
Veget.	3020	712	2	11989	31.1

Table 5: Confusion matrix for test data using 60 trees and 4 split variables. Total error rate=4.99%, 5×5 window size

Figure 4 shows the corresponding classification result.

When increasing the neighborhood size, classification results are only enhanced for the building class, but are worse for all the other classes. In fact, buildings can be represented by large homogeneous segments with regard to lidar features. Therefore when dealing with larger neighborhoods, the training pixels have more representative mean values. It is similar for the artificial ground class however due to some small roads between buildings, the large neighborhood may include building points which increases the number of artificial ground pixels that are misclassified to building class (*cf.* Table 5). The total error rate seems to be smaller with a large neighborhood, however this is due to the fact that building class has the higher number of pixels.

4.4.2 Variable Importance of selected features The variable importance was reprocessed for the 17 selected features in order to study more precisely the relevant features for each class. Two data sets were used with different window sizes: 3×3 (*cf.* Figure 5) and 5×5 (*cf.* Figure 6).

Firstly, one can observe that the variable importance values are higher and better distinguished when using a small window size since training pixels are more homogeneous. Secondly, when using a large window size, pixels may be mixed in the neighborhood, many variables give the same importance (*cf.* Figure. 6) for all classes which reveals the classification ambiguity. Consequently, the variable importances seem to be more reliable with a small neighborhood size. It will be discussed hereby.

We confirm that the height difference is the most important feature for all classes, which is the only topographic variable. For artificial ground, considering the different group features, the most important attributes are: P_λ for planarity, D_Π since it is a flat surface. FW selected attributes seem to have the same importance for this class. As for building class, the most important features in different groups are: S_λ,N_z and A. For plane-based features, the distance to the plane D_Π is more sensitive to the scan trajectory (the plane is better estimated along the scan trajectory since there are more points) and to the roof area (a large roof returns a higher distance to plane). For this reason it is less important than the deviation angle. For natural grounds, many variables seem to be important. This result should be interpreted with caution due to the few number of corresponding training samples. Finally, for vegetation pixels, the most relevant features of each group are: S_λ as it returns isotropic local distribution, R_z since no robust plane can be fitted to vegetation and finally the echo width w as already stated in (Wagner et al., 2008). For the latter classes, variable importance seems to be more dispersed between different attributes. This dispersion is correlated to the higher error rates on both classes (*cf.* Table 4).

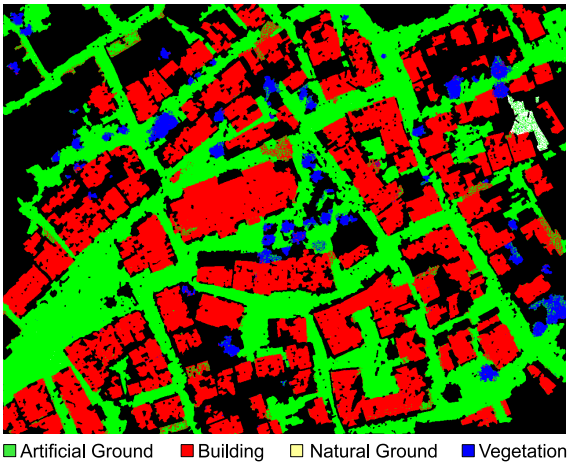

(a) Classification results - Lidar Features : 5×5 window size

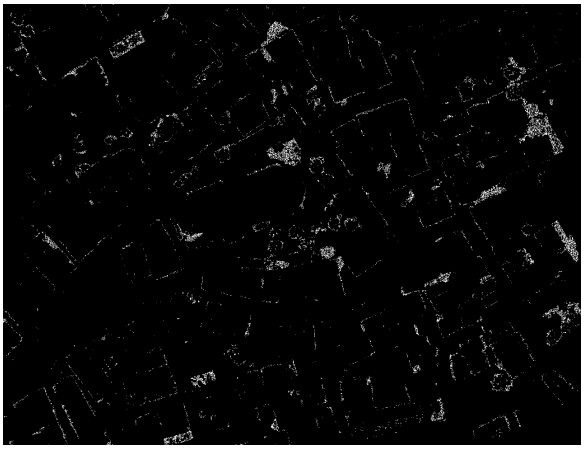

(b) Difference with the ground truth

Figure 4: Classification result (T=60 trees and M=4.)

4.4.3 Computing time The computing time for feature selection process (21 features) to 17 selected lidar features is 367 minutes. This value is not critical since the feature selection is done only one time provided a set of input attributes. The classification process for 17 lidar selected features needs 11.36 minutes. Random Forests do not need an intensive computing time, however a considerable amount of memory is needed to store a N by T matrix in memory.

5 CONCLUSION

In this work, Random Forests were successfully applied to the lidar feature selection to classify urban scenes. 21 lidar features were proposed and separated into five groups: height-based, echo-based, eigenvalue-based, plane-based and FW features. The method is a decision tree based ensemble classifier. It provides accurate classification and a variable importance estimate based on the permutation accuracy criteria. A feature selection was processed by iterative backward feature elimination. A minimal feature vector with 6 features provides a low OOB error rate. The most relevant feature for all classes is the height difference. Echo-based attributes seem to be non-relevant.Two FW features A and W appear in the final set, which confirms the contribution of full-waveform lidar for urban scene classification. The 2D window size impact on variable importance has been studied. Small sizes should be used to enhance the feature discrimination and to improve classification accuracy. Some non-relevant lidar features in our context, should be more useful for a finer classification such

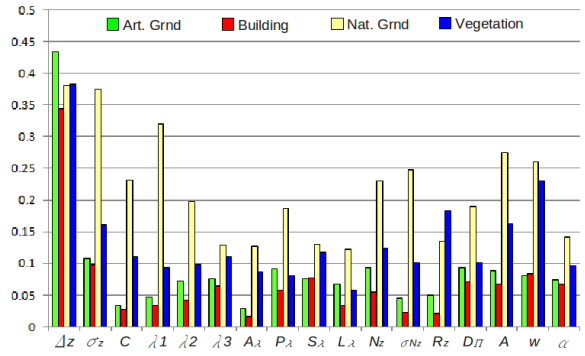

Figure 5: Variable importance per class - 3×3 window size

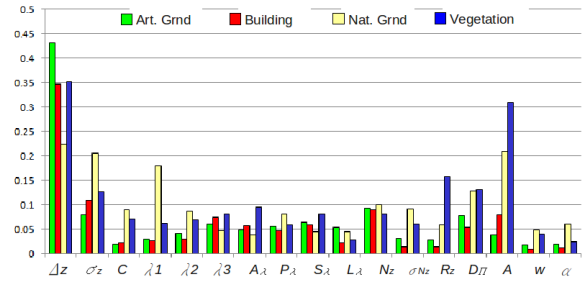

Figure 6: Variable importance per class - 5×5 window size

as the deviation angles for roof segmentation.

ACKNOWLEDGEMENTS

The Random Forests implementation software by L. Breiman and A. Cutler was used in experiments. For this work, we used the R interface of the software which is distributed freely on `http://www.r-project.org`.

REFERENCES

Breiman, L., 2001. Random forests. Machine Learning 45(1), pp. 5–32.

Breiman, L., Friedman, J., Olshen, R. and Stone, C., 1984. Classification and regression trees. Chapman & Hall, New York.

Briem, G., Benediktsson, J. and Sveinsson, J., 2002. Multiple classifiers applied to multisource remote sensing data. IEEE Transactions on Geoscience and Remote Sensing 40(10), pp. 2291–2999.

Charaniya, A., Manduchi, R. and Lodha, S., 2004. Supervised parametric classification of aerial lidar data. In: Real-Time 3D Sensors and their Use Workshop, in conjunction with IEEE CVPR, pp. 30–37.

Chauve, A., Mallet, C., Bretar, F., Durrieu, S., Pierrot-Deseilligny, M. and Puech, W., 2007. Processing full-waveform lidar data: modelling raw signals. International Archives of Photogrammetry, Remote Sensing and Spatial Information Sciences 36 Part 3/W52, pp. 102–107. Espoo, Finland.

Díaz-Uriarte, R. and de Andrés, S. A., 2006. Gene selection and classification of microarray data using random forest. BMC BioInformatics, 7(3).

Ducic, V., Hollaus, M., Ullrich, A., Wagner, W. and Melzer, T., 2006. 3D Vegetation mapping and classification using full-waveform laser scanning. In: EARSeL and ISPRS Workshop on 3D Remote Sensing in Forestry, Vienna, Austria, pp. 211–217.

Gislason, P., Benediktsson, J. and Sveinsson, J., 2006. Random forests for land cover classification. Pattern Recognition Letters 27(4), pp. 294–300.

Gross, H. and Thoennessen, U., 2006. Extraction of lines from laser point clouds. In: ISPRS Conference Photogrammetric Image Analysis (PIA), Vol. 36 Part 3A, IAPRS, Bonn, Germany, pp. 87–91.

Gross, H., Jutzi, B. and Thoennessen, U., 2007. Segmentation of tree regions using data of a full-waveform laser. In: ISPRS Conference Photogrammetric Image Analysis (PIA), Vol. 36, IAPRS, Munich, Germany.

Haala, N. and Brenner, C., 1999. Extraction of buildings and trees in urban environments. ISPRS Journal of Photogrammetry & Remote Sensing 54(2-3), pp. 130–137.

Mallet, C., Bretar, F. and Soergel, U., 2008. Analysis of full-waveform lidar data for classification of urban areas. Photogrammetrie Fernerkundung GeoInformation (PFG) 5, pp. 337–349.

Matikainen, L., Kaartinen, H. and Hyyppä, J., 2007. Classification tree based building detection from laser scanner and aerial image datas. International Archives of Photogrammetry, Remote Sensing and Spatial Information Sciences 36 (Part 3/W52), pp. 280–287.

Pal, M., 2005. Random Forest classifier for remote sensing classification. International Journal of Remote Sensing 26(1), pp. 217–222.

Rottensteiner, F., Trinder, J., Clode, S. and Kubik, K., 2005. Using the dempster-shafer method for the fusion of lidar data and multi-spectral images for building detection. Information Fusion 6(4), pp. 283–300.

Secord, J. and Zakhor, A., 2007. Tree detection in urban regions using aerial lidar and image data. IEEE Geoscience and Remote Sensing Letters 4(2), pp. 196–200.

Sithole, G. and Vosselman, G., 2004. Experimental comparison of filter algorithms for bare-earth extraction from airborne laser scanning point clouds. ISPRS Journal of Photogrammetry and Remote Sensing 59(1-2), pp. 85–101.

Steinle, E. and Vögtle, T., 2001. Automated extraction and reconstruction of buildings in laserscanning data for disaster management. In: Proc. of the Workshop on Automatic Extraction of Man-Made Objects from Aerial and Space Images, Ascona, Switzerland.

Strobl, C., Boulesteix, A.-L. and Augustin, T., 2007. Unbiased split selection for classification trees based on the Gini index. Computational Statistics & Data Analysis 52(1), pp. 483–501.

Wagner, W., Hollaus, M., Briese, C. and Ducic, V., 2008. 3D vegetation mapping using small-footprint full-waveform airborne laser scanners. International Journal of Remote Sensing 29(5), pp. 1433–1452.

Wagner, W., Ullrich, A., Ducic, V., Melzer, T. and Studnicka, N., 2006. Gaussian decomposition and calibration of a novel small-footprint full-waveform digitising airborne laser scanner. ISPRS Journal of Photogrammetry & Remote Sensing 60(2), pp. 100–112.

Xu, G. and Zhang, Z., 1996. Epipolar Geometry in stereo, motion and object recognition. Kluwer Academic Publishers.